IOP Publishing

Principles of Biophotonics, Volume 2
Light emission, detection, and statistics
Gabriel Popescu

Chapter 12

Semiconductor materials

12.1 Insulators and conductors

Photodetection is the process by which light is converted into a measurable quantity, typically an electrical signal. For example, the optical radiation can induce changes in the detector material such as resistance or inductance, which in turn produce changes in the measured current through or voltage across the detector (figure 12.1). During the detection process, a part of the incident optical power is converted into electrical power. Thus, photodetection is a *dissipative* process. In other words, if the light interacts with the material without exchange of energy, that is, *elastically*, detection is not possible.

Light–matter interaction is governed by the displacement of electronic charge that the optical field induces into the material. The incident light on a material applies an electric force on the electrons in that material,

$$\mathbf{F} = -e\mathbf{E}. \tag{12.1}$$

In equation (12.1), $-e$ is the charge of the electron and $\mathbf{E}$ is the electric field carried by the optical radiation. Figure 12.2 illustrates the interaction between the light and a *dielectric* (insulator) material. Insulators (e.g. glass) contain electrons tightly bound to the nuclei and the perturbation induced by the incident optical field happens without loss of energy. The electron behaves as a mass on a spring, with the electric force exerted by the nucleus acting as the restoring force. As a result, the incident light is re-radiated by the material with 100% of the original power recovered as transmitted or reflected light. This process explains why good dielectric materials are also transparent to electromagnetic radiation.

For *conductive* materials, the situation is rather different. In an ideal conductor, which is approximated well by a *metal*, electrons are free to move around. The binding to the nuclei is so weak ($F_N \cong 0$) that the electrons can be considered as a gas, moving unrestricted in the material. As a result, the electrons are accelerated by the incident optical field and undergo collisions with the atoms in the lattice

doi:10.1088/978-0-7503-1644-6ch12

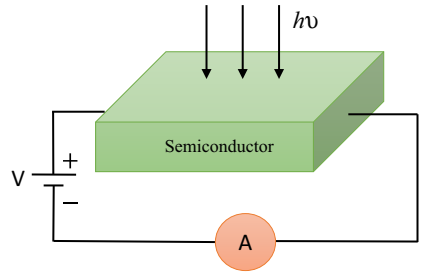

Figure 12.1. An example of photodetection mechanism whereby the incident light produces a change in the measured voltage across the detector or current flow.

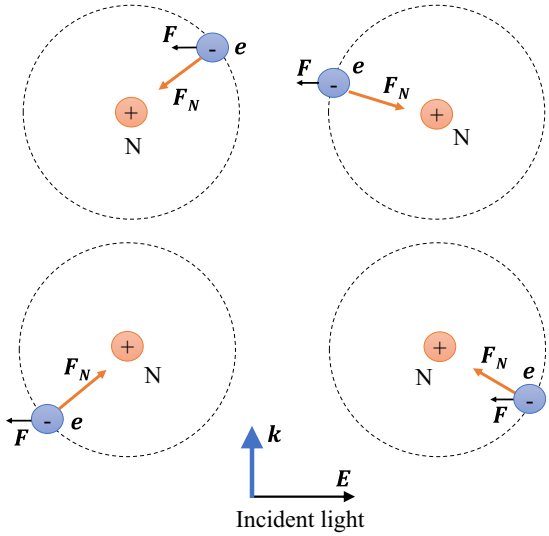

Figure 12.2. Interaction of the optical field, $\boldsymbol{E}$, wavevector $\boldsymbol{k}$, with an *insulator* (dielectric). Electrons (−) are bound strongly to the nuclei (+) by Force $\boldsymbol{F}_N$, such that the electric force, $\boldsymbol{F}$, applied by the incident field is unable to break them away. The light–matter interaction is *elastic* (no loss).

(figure 12.3). During the collision process, electrons transfer some of their energy to the vibrational modes of the lattice, which, eventually, converts into heat. Thus, the interaction of light with conductors is a *dissipative* process. This description explains why good conductors, such as metals, are generally *opaque* to electromagnetic radiation.

Semiconductors are materials with conductivity that falls between that of metals and insulators. Because their electrical properties can be tuned with respect to temperature, concentration of impurities, voltage bias, etc, semiconductors are commonly used in photodetectors. Next, we discuss the basic properties of semiconductor materials (for a classical reference on semiconductor devices, see [1]).

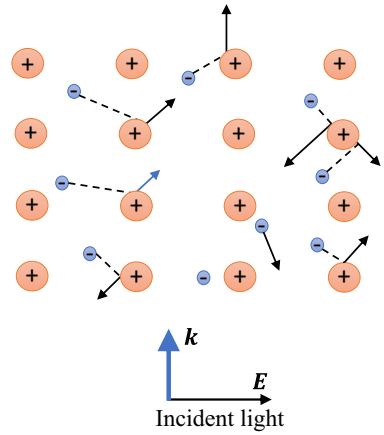

Figure 12.3. Interaction of light with a conductor. Electrons are free to move in the lattice and are accelerated by the electric field of incident light. Due to collisions with the ions in the lattice, electrons dissipate into heat some of the field energy.

12.2 Covalent bonds in semiconductor crystals

Semiconductors are solids in *crystalline form*, meaning that their atoms and molecules are arranged spatially in a regular and periodic manner (for a physical description of crystals, see [2]). A highly ordered three-dimensional distribution of atoms or molecules is known as a *crystal lattice*. In semiconductors, the atoms are held together by *covalent bonds*, in which pairs of electrons are shared between atoms (see figures 12.4 and 12.5).

Silicon (Si) and Germanium (Ge) are the most commonly used semiconductor materials. Both materials have four valence electrons, that is, four electrons on their outer, incomplete electronic shell. Silicon (Si, atomic number $Z = 14$) has a total of 14 electrons, 10 of which form complete shells ($1s^2 2s^2 2p^6 3s^2 3p^2$, in orbital notation). Germanium (Ge, $Z = 32$) has 32 electrons, 28 of which form complete shells ($1s^2 2s^2 2p^6 3s^2 3p^6 3d^{10} 4s^2 4p^2$, in orbital notation). The two electronic configurations are shown in figure 12.4.

Germanium's valence electrons exist on higher energy levels (farther from the nucleus) than those of silicon. As a result, the Ge electrons are more mobile, resulting in higher conductivity compared to Si.

Figure 12.5 illustrates how a Si atom can form covalent bonds with four other atoms, sharing a total of four pairs of electrons and, thus, creating a complete shell of electrons.

12.3 Energy band structure

The atomic model put forward by Niels Bohr in 1913 correctly explained the discrete spectral lines measured from the hydrogen atom. Bohr's atom consists of a condensed nucleus surrounded by revolving electrons, as illustrated in figures 12.4(a) and (b). However, this discrete occupancy of energy levels is not limited to isolated atoms. The covalently bound atoms in a semiconductor also

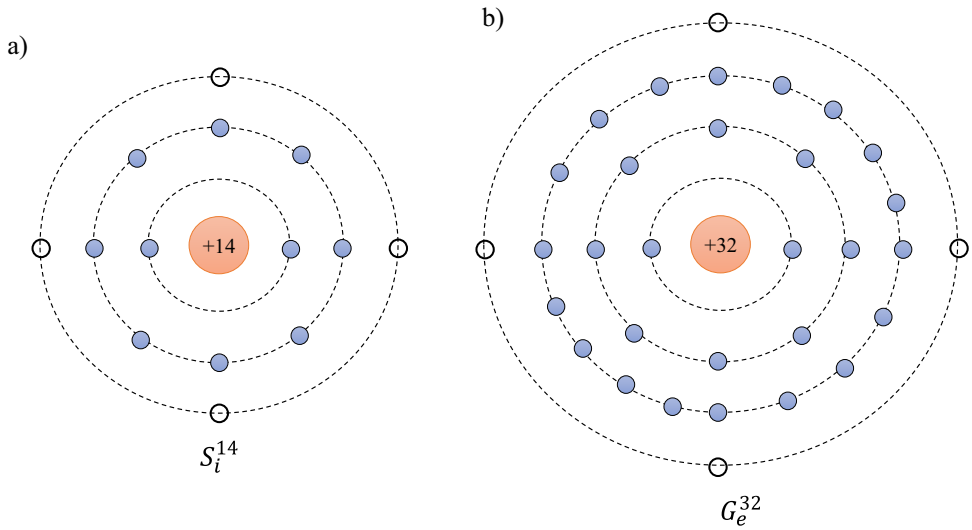

Figure 12.4. a) Electronic structure of Silicon (Si). Si has three electronic shells: $1s^2$ (two electrons), $2s^2$ $2p^6$ (eight electrons), $3s^2$ $3p^2$ (four electrons). b) Electronic structure of germanium (Ge). Ge has four electronic shells: $1s^2$ ($2\bar{e}$), $2s^2$ $2p^6$ ($8\bar{e}$), $3s^2$ $3p^6$ $3d^{10}$ ($18\bar{e}$), and $4s^24p^2$ ($4\bar{e}$). Both materials have four valence electrons, depicted by empty circles.

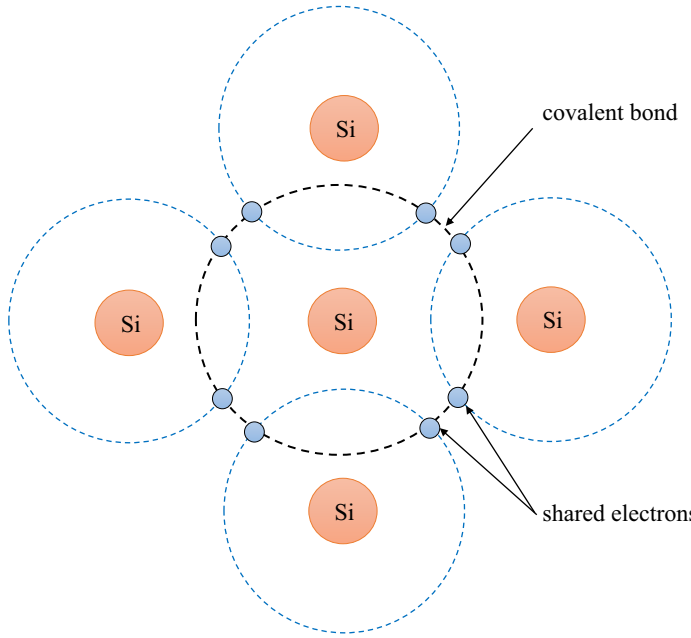

Figure 12.5. Illustration of the covalent bond in crystalline silicon. Pairs of electrons from the outermost shells are shared by an atom with four other atoms, creating a stable electronic shell (eight electrons).

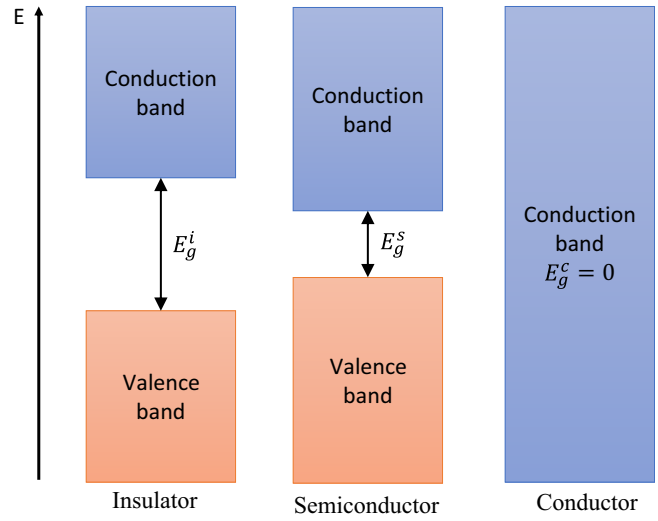

Figure 12.6. Energy band structure for insulators, semiconductors and conductors. The bandgap energy is much higher for insulators vs semiconductors, $E_g^i > E_g^s$, and non-existent for conductors, $E_g^c = 0$.

create discrete energy levels. However, unlike with isolated atoms, in a semiconductor crystal the energy levels are lumped into two bands: the *valence* and the *conduction* band (for a review of solid-state physics, see [3]).

The valence bond contains many closely packed energy levels. The two bands are separated by a *forbidden* energy region, containing no allowed energy levels, referred to as the *band gap*. The electrons in the valence band are tightly bound to the atoms, behaving as in an insulator (recall figure 12.2). They need to receive an energy at least equal to the bandgap to become free to move, that is, to transition to the conduction band. Thus, the electrons in the conduction band are loosely bound and virtually free to move around, like in a conductor (recall figure 12.3).

This energy band structure is not particular to only semiconductors, as conductors and dielectrics also have their own versions. What distinguishes the three types of materials is the energy necessary to move an electron from the valence to the conduction band, that is, the size of the *bandgap*. Thus, the insulators have a very large bandgap, while for an ideal conductor, the bandgap is non-existent (see figure 12.6).

When an electron transitions from a bound to free state, that is, when it moves from the valence to the conduction band, it leaves behind a net positive charge. This positive charge is referred to as a *hole*. The hole is not an actual particle containing a localized positive charge, but, rather, a fictitious particle defined by the absence of a negative charge. However, the concept of a hole is useful in describing charge transport in semiconductors.

12.4 Carrier distribution

Previously, when describing the black body radiation, we found that photons, being non-interacting, indistinguishable particles, or *bosons*, obey the Bose–Einstein

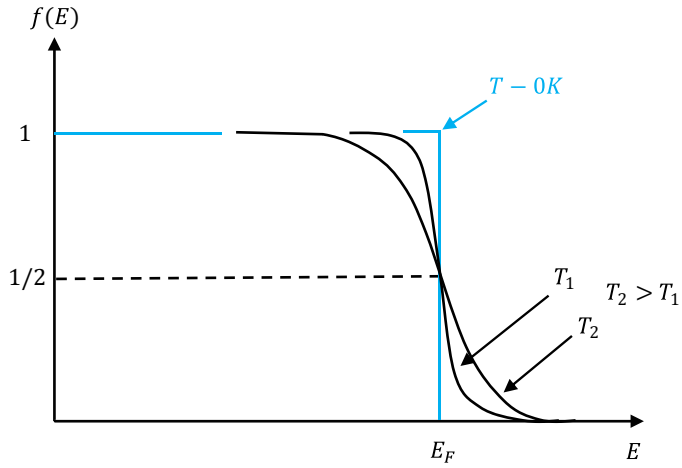

Figure 12.7. The Fermi–Dirac distribution.

statistics (see section 6.1). Thus, the probability of occupancy for a mode of energy $h\nu$ has the form (see Planck's formula in equation (6.2) and [4])

$$f(\nu) = \frac{1}{e^{\frac{h\nu}{k_B T}} - 1} \tag{12.2a}$$

where, as usual, k_B is the Boltzmann constant and T the absolute temperature. However, the energy distribution of electrons in a semiconductor is quantitatively different. Unlike photons, electrons obey Pauli's exclusion principle, which states that it is impossible for two electrons in an atom to have the same values of the four quantum numbers (principal quantum number, n, angular momentum quantum number, ℓ, magnetic quantum number, m_e, and m_s the spin quantum number). We discussed in section 5.1 how the electron spin defines the electronic state as a singlet, doublet or triplet.

Electrons belong to the family of *fermions*, particles that carry half-integer spin (note that photons have spin 1). As a result, the occupancy of the energy levels is governed by the Fermi–Dirac statistics (figure 12.7),

$$f(E) = \frac{1}{e^{\frac{(E - E_F)}{k_B T}} + 1}. \tag{12.2b}$$

In equation (12.2*b*), E_F denotes the *Fermi level*. To gain a physical understanding of the Fermi level, it is informative to study the case of $T \to 0$:

$$\lim_{T \to 0} e^{\frac{E - E_F}{k_B T}} = \begin{vmatrix} 0, & if\ E < E_f \\ \infty, & if\ E > E_f \end{vmatrix}. \tag{12.3}$$

Therefore, the occupancy probability at $T = 0\ K$ has the asymptotic values

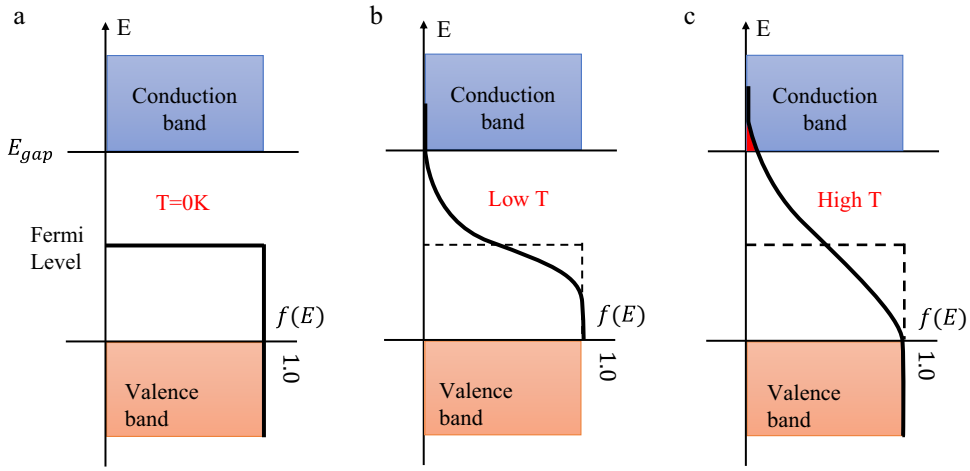

Figure 12.8. The Fermi distribution overlaid with the energy bands of an intrinsic semiconductor. (a) $T = 0$ K: no energy allowed above the Fermi level. (b) Low temperatures: energy levels above the Fermi level; only a few in the conduction band. c) High temperatures: some energy levels exist in the conduction band.

$$\lim_{T\to 0} f(E) = \begin{vmatrix} 1, & if\ E < E_f \\ 0, & if\ E > E_f \end{vmatrix}. \tag{12.4}$$

Equation (12.4) provides an insightful description of the Fermi level: it is the maximum energy occupied at absolute zero temperature. For intrinsic semiconductors, containing an equal number of positive and negative charge carriers, the Fermi level lies in the middle of the bandgap. This is the level at which the probability of occupancy is ½, $f(E_F) = 1/2$, meaning that the probability of occupancy at this energy level is ½. For silicon, $E_g = 1.12\,eV(1.79 \cdot 10^{-19}\ \text{J})$, which indicates that the Fermi level lies $0.56\,eV$ above the valence band. For comparison, the thermal energy at room temperature is only $k_B T = 0.026\,eV$. This indicates that at $T = 300$ K, the probability of occupancy for energy levels $E > E_F$ is very low.

To gain a better understanding of the temperature effect, figure 12.8 shows $f(E)$ overlaid with the energy bands for a semiconductor, at zero, low, and high temperatures. The illustration in figure 12.8 provides information about the conductive properties of the semiconductor. Since there is a gap between the Fermi level and the conduction band, there will be absolutely no energy levels allowed in the conduction band at $T = 0$ K. It is important to note that even though $f(E)$ has finite values within the gap, there are still no electrons occupying those states, consistent with the definition of the gap. In order to understand this better, we calculate the number of particles per unit volume, $n(E)$, with energy within the interval $(E,\ E + dE)$. This quantity can be expressed as

$$n(E)dE = \rho(E)f(E)dE. \tag{12.5}$$

In equation (12.5), $\rho(E)$ is the density of states, meaning the number of energy states per unit volume within $(E,\ E + dE)$, while $f(E)$ is the Fermi distribution

(equation (12.2b)). In order to calculate the density of states, we start by evaluating the number of modes in a cavity of volume V. Following the same reasoning as in section 6.1, the number of modes per wavenumber interval is (equation 6.15, chapter 6)

$$dN = \frac{V}{2\pi^2} k^2 \, dk. \tag{12.6}$$

To change the variable from wavenumber to energy, we use the relationships from quantum mechanics,

$$E = \frac{p^2}{2m} \tag{12.7a}$$

$$\mathbf{p} = \hbar \mathbf{k} \tag{12.7b}$$

where $\mathbf{p}$ is the momentum of the electron, $p = [\mathbf{p}]$, m its mass, and $\hbar = h/2\pi$ the reduced Planck's constant. Combining equations (12.7*a* and *b*), we obtain the following $k-E$ relationship

$$k = \left(\frac{2mE}{\hbar^2} \right)^{1/2} \tag{12.8a}$$

$$dk = \frac{1}{\hbar} \sqrt{\frac{2m}{E}} \, dE. \tag{12.8b}$$

If we now plug equations (12.8*a* and *b*) into equation (12.6), we obtain

$$\begin{aligned} dN &= \frac{V}{2\pi^2} \frac{2mE}{\hbar^2} \frac{1}{\hbar} \sqrt{\frac{2m}{E}} \, dE \\ &= \frac{4\pi (2m)^{3/2}}{h^3} V \sqrt{E} \, dE. \end{aligned} \tag{12.9}$$

Thus, we can now express the density of states present in equation (12.5) as

$$\begin{aligned} \rho(E) &= \frac{1}{V} \frac{dN}{dE} \\ &= \frac{4\pi (2m)^{3/2}}{h^3} \sqrt{E}. \end{aligned} \tag{12.10}$$

Using equations (12.5) and (12.10), we can now express the number of particles in the conduction band per unit volume and energy within the interval $(E, \; E + dE)$, namely, $n(E) = \rho(E) f(E)$. Semiconductor and conductor materials are of course, characterized by the same Fermi distribution, $f(E)$. However, the density of states for semiconductors is at the top of the gap, in other words, ρ is shifted by the bandgap energy, E_g. For a conductor, the density of states starts at the

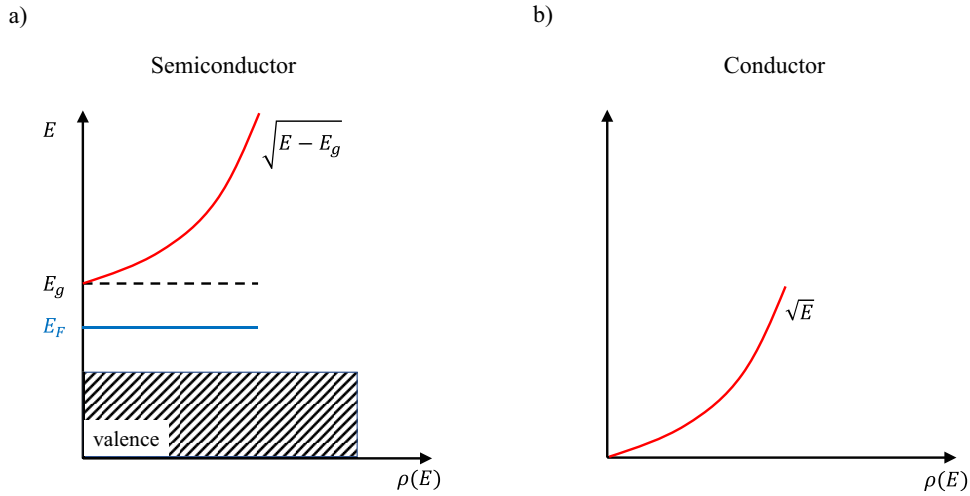

Figure 12.9. Density of states starts at the top of the bandgap for a semiconductor (a), and at the bottom of the valence band for a conductor (b).

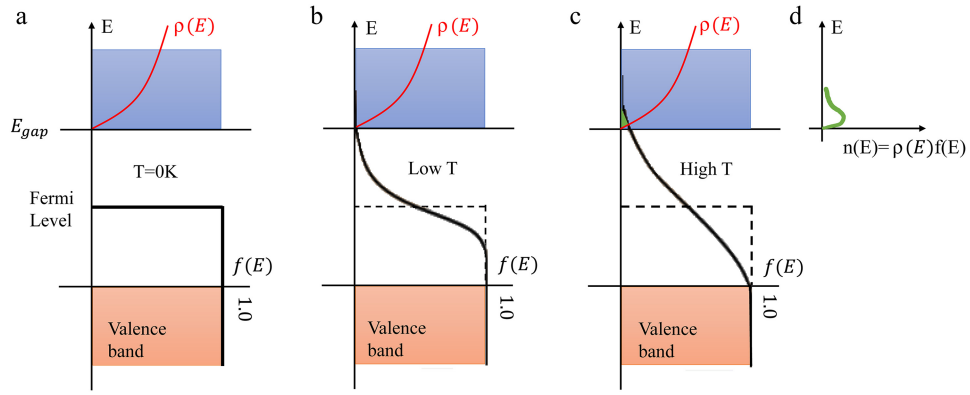

Figure 12.10. (a–c) Multiplying the density of states (figure 12.8) with the Fermi distribution yields the carrier distribution (electron population), $n(E)$. (d) Carrier distribution for the high temperature situation shown in (c).

bottom of valence band (see figure 12.9). Thus, we have the following expressions for the electron population in the conduction band

$$n(E) = \frac{4\pi(2m)^{3/2}}{h^3}\frac{1}{e^{\frac{E-E_F}{k_BT}}+1}\sqrt{E-E_f}\,, \text{ for semiconductors} \qquad (12.11a)$$

$$n(E) = \frac{4\pi(2m)^{3/2}}{h^3}\frac{1}{e^{\frac{E-E_F}{k_BT}}+1}\sqrt{E}\,, \text{ for conductors.} \qquad (12.11b)$$

Finally, we are ready to update figure 12.7 with the electron population curves, as shown in figure 12.10(d).

In order to find out the total number of electrons in the conduction band, n_c, we integrate $n(E)$ from the bottom of the conduction band to infinity,

$$n_c = \int_{E_g}^{\infty} n(E)dE. \tag{12.12}$$

For silicon and germanium at energies in the conduction band, the following inequality holds, $E - E_F \geqslant k_B T$. This approximation is well justified if we note that, at room temperature ($T = 300k$)

$$k_B T = 0.026\, eV \tag{12.13a}$$

$$E_g^{Si} = 1.1\, eV \tag{12.13b}$$

$$E_g^{Ge} = 0.67\, eV. \tag{12.13c}$$

As a result of this approximation, $e^{\frac{E-E_F}{k_B T}} + 1 \simeq e^{\frac{E-E_F}{k_B T}}$, and

$$\begin{aligned} \frac{1}{e^{\frac{E-E_F}{k_B T}} + 1} &\simeq e^{-\frac{(E-E_F)}{k_B T}} \\ &= e^{-\frac{E_g}{2k_B T}}. \end{aligned} \tag{12.14}$$

In equation (12.14), we used the fact that, for an intrinsic semiconductor, E_F lies in the middle of the bandgap and $E - E_F = E_g/2$. With this approximation, equation (12.11*a*) simplifies to

$$n(E) = \frac{4\pi(2m)^{3/2}}{h^3} e^{-\frac{E_g}{2k_B T}} \sqrt{E - E_f}\,. \tag{12.15}$$

Integrating over the energy, equation (12.12) yields for the electron concentration in the conduction band,

$$n_c = AT^{3/2} e^{-E_g/2k_B T} \tag{12.16a}$$

$$\begin{aligned} A &= \frac{2(2\pi m k_B)^{3/2}}{h^3} \\ &= 4.83 \times 10^{21}\, \frac{\text{electrons}}{\text{m}^3\text{k}^{3/2}}. \end{aligned} \tag{12.16b}$$

Equations (12.16*a–b*) show that, at room temperature, Si has $n_c^{Si} = 1.4 \times 10^{16}$ electrons/m^3. On the other hand, Ge has $n_c^{Ge} = 5.9 \times 10^{19}$ electrons/m^3, a significantly larger number.

12.5 Doping

So far, we described the energy band structures and carrier distributions for *ideal* semiconductors. These materials are assumed to be free of impurities. This class of semiconductors are called *intrinsic.* In such materials, the electrons and holes are

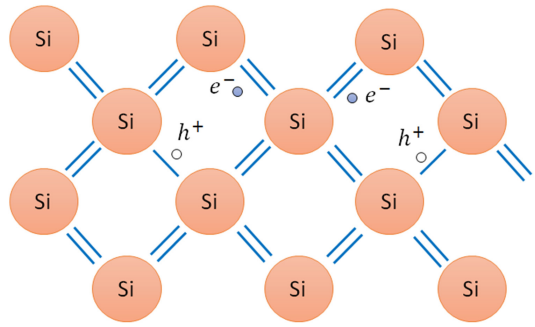

$$n = p = n_i$$

Figure 12.11. Electron–hole pairs in a Si crystal: e^-, electron, h^+, hole. The concentration of electrons is equal to that of holes in an intrinsic semiconductor.

created in pairs. Thus, the concentration of electrons (n) in the conduction band equals that of the holes (p) in the valence band,

$$n = p = n_i \tag{12.17}$$

where n_i is the carrier concentration for an intrinsic semiconductor. Figure 12.11 illustrates the electron–hole pair (EHP) generation in an intrinsic semiconductor.

Recombination is the reverse process of EHP *generation*. The rate of generation, g_i, $[g_i]$ = EHP/m^{3}s and of recombination, r_i, $[r_i]$ = EHP/m^{3}s, must be equal, at any temperature. The rate of recombination is proportional to the equilibrium concentrations of both electrons (n_0) and holes (p_0),

$$\begin{aligned} r_i &= cn_0p_0 \\ &= cn_i^2 \\ &= g_i, \end{aligned} \tag{12.18}$$

where c is a proportionality constant that depends on the specifics of the recombination process.

The electrical properties of semiconductors can be modified to accomplish particular tasks if impurities are added to the intrinsic material. This process is referred to as *doping* and is the most common method for tuning the conductivity of semiconductors. Through doping, a material receives either an excess of electrons, thus becoming an *n-type* material, or excess of holes, for a *p-type* material. As a result, the equilibrium concentrations, n_0, p_0, no longer equal the intrinsic carrier concentration, n_i.

N-type semiconductors are typically obtained by adding impurities from column V of the periodic table (figure 12.12a). These elements have five electrons on their outer shell, of which only four can form covalence bonds with the crystal (recall figure 12.5). Therefore, the fifth electron is weakly bound and can participate in conduction. These elements from column V are called *donor impurities*, because they contribute free electrons to the material.

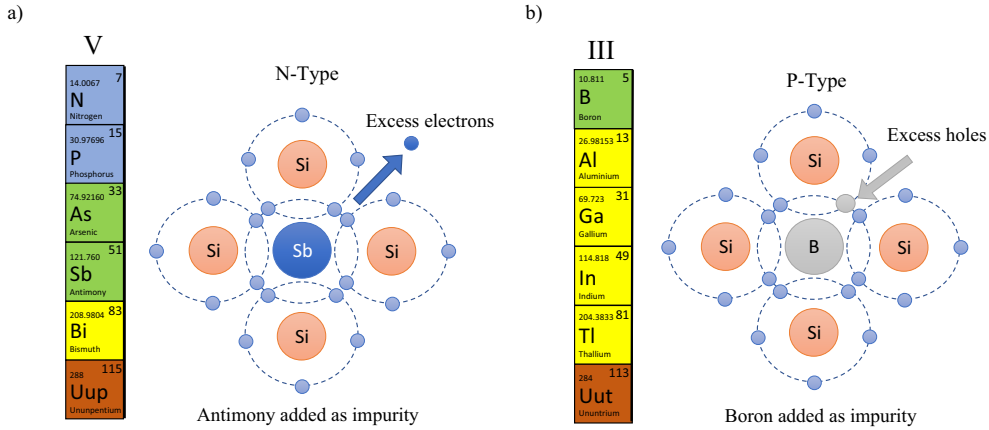

Figure 12.12. (a) N-type semiconductors are obtained by adding impurities from column V of the periodic table. These elements contribute free electrons. (b) P-type semiconductors are doped with elements from column III, which create holes.

P-type semiconductors are obtained by doping with elements from column III of the periodic table (figure 12.12b). In this case, the three electrons on the outer shell of these atoms are not sufficient to create the covalent bonds with the crystal. Thus, one bond remains incomplete as it misses one electron, or possesses an extra hole. We anticipate that in p-type semiconductors, there is excess of hole concentration (p) in the *valence* band.

Doping brings modifications to the band diagram, density of states, Fermi–Dirac distributions, and the carrier concentrations (see figure 12.13). For an n-type material (figure 12.13b), due to the excess of electrons, the Fermi level is shifted up, closer to the conduction band. As a result, the electron concentration is increased in the conduction band, at the expense of the hole concentration in the valence band. In p-type semiconductors, the Fermi level is shifted down, such that the hole concentration is increased in the valence band. The electron concentration in the conduction band is reduced.

12.6 Electron–hole pair generation by absorption of light

The fundamental process involved in photodetection is the generation of EHPs through absorption of radiation. These EHPs are often called *excess carriers*, indicating that they add to the existing carrier concentration at thermal equilibrium. Since the generated EHPs are out of equilibrium with their environment, they must eventually recombine.

As illustrated in figure 12.14, a photon with energy above the bandgap of the material, $h\nu > E_g$, can be absorbed, creating an electron in the conduction band and one hole in the valence band. As the valence band contains available electrons and the conduction band has numerous available energy states, the absorption process has high probability. The electron excited to the conduction band may have an energy higher that most electrons and will eventually lose this excess energy via

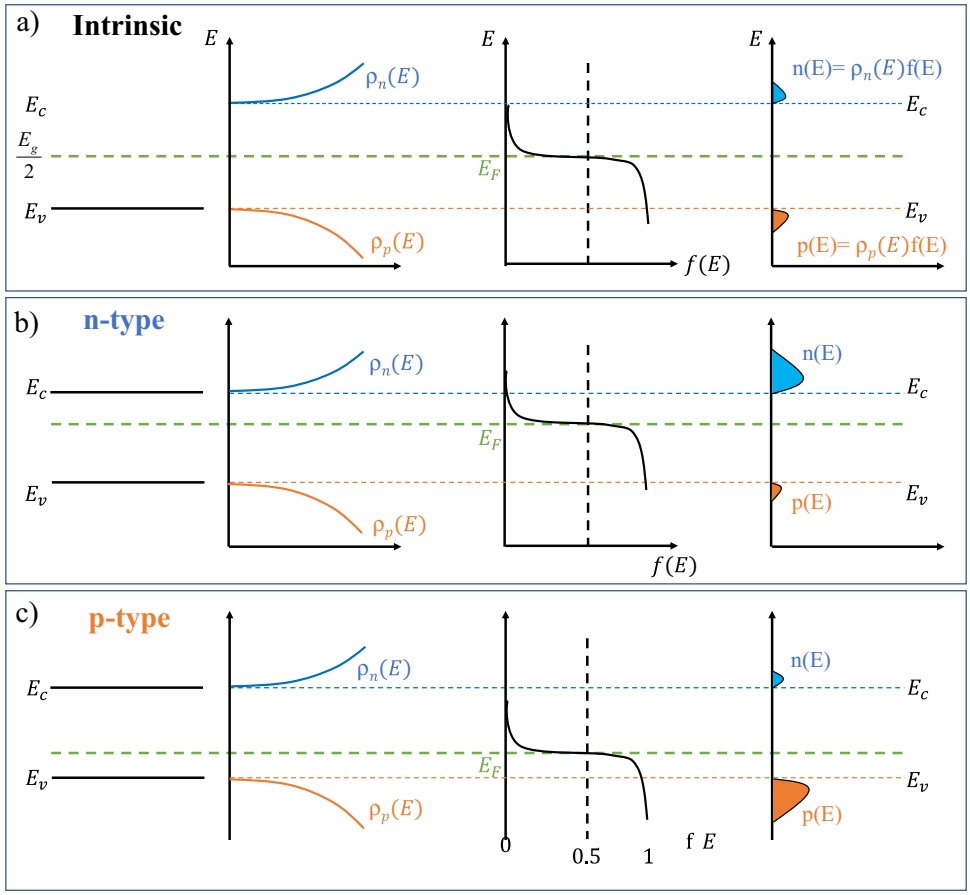

Figure 12.13. Band diagram, density of states (ρ), Fermi–Dirac distribution (f), and the carrier concentrations (n, p): (a) intrinsic, (b) n-type, and (c) p-type semiconductors at thermal equilibrium.

scattering with the lattice. This dissipative process excites vibrations in the lattice, which eventually converts into heat. As a result, the electron will lower its velocity and reach an energy level close to E_c. Finally, the electron can *recombine* with a hole in the valence band. This recombination process can be accompanied by the emission of a photon, a process called *photoluminescence*. Luminescence can also occur as a result of material bombardment with high-energy electrons (*cathodoluminescence*) or running a current through the material (*electroluminescence*). Photons with energies below the bandgap cannot excite electrons to the conduction band and, thus, are not absorbed. The semiconductor is *transparent* to photons of energies $h\nu < E_g$ and cannot act as detector at these wavelengths.

Let us consider a plane wave of *photon irradiance* I_q^0(in s^{-1}/m^2) incident on to a semiconductor of thickness L (figure 12.15). The change in I_q due to the absorption in a slice of thickness dz is proportional with the photon irradiance at the slice, $I_q(z)$, and the thickness of the slice,

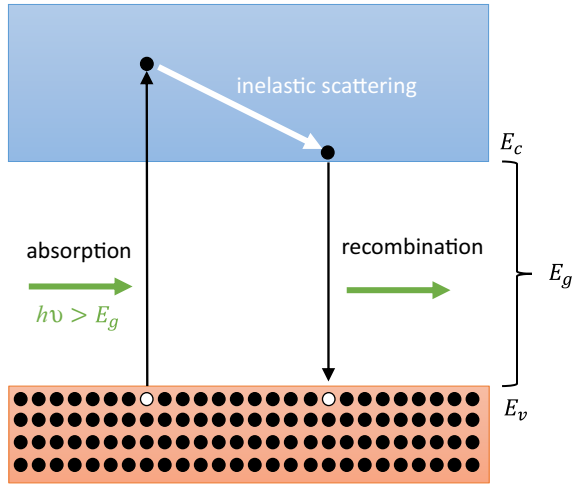

Figure 12.14. Optical absorption of a photon with energy higher than the bandgap creates an EHP. The electron excited in the conduction band loses energy via inelastic scattering with the lattice and occupies a lower energy level in the conductance band. Finally, the electron recombines with a hole in the valence band and can produce photoluminescence.

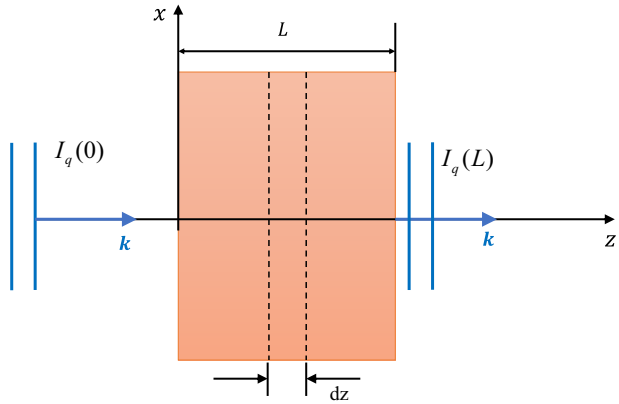

Figure 12.15. Lambert–Beer law for absorption of light in a material of thickness L.

$$dI_q(z) = -\alpha I(z)dz. \tag{12.19}$$

In equation (12.19), the proportionality constant, α, is called the *absorption coefficient* and the negative sign denotes a decrease in I_q with propagation, as expected. To obtain the photon irradiance at the exit surface of the material, $z = L$, we integrate equation (12.19),

$$\int_0^L \frac{dI_q(z)}{I_q(z)} = -\alpha z \Big|_0^L, \tag{12.20}$$

which yields

$$I_q(L) = I_q(0)e^{-\alpha L}. \tag{12.21}$$

Equation (12.21) represents the Lambert–Beer law of absorption.

Note that the absorption coefficient (units of m^{-1}) has a wavelength dependence that depends on the material. As discussed, we expect very low absorption for photon energies below the bandgap. Figure 12.16(a) illustrates the α versus $h\nu$ dependence and figure 12.16(b) shows the bandgap energies for various materials and the corresponding wavelengths. There is a useful relationship that connects the photon energy in units of eV and its wavelength,

$$E(\text{eV}) = \frac{1.24}{\lambda(\mu\text{m})}. \tag{12.22}$$

As shown in figure 12.16(b), many materials have bandgap energies below the visible range. For example, Si has a bandgap $E_g^{\text{Si}} = 1.17\text{eV}$, which corresponds to

$$\begin{aligned}\lambda_g^{\text{Si}} &= \frac{1.24}{1.17}\mu\text{m} \\ &= 1.06\ \mu\text{m}.\end{aligned} \tag{12.23}$$

Thus, Si makes an excellent photodetector material for visible light $\lambda \in (0.4, 0.75)\ \mu\text{m}$, but becomes essentially transparent for $\lambda > 1\ \mu\text{m}$. Germanium, on the other hand, has a smaller bandgap, $\lambda_g^{\text{Ge}} = 0.67\ \text{eV}$; this can detect longer wavelengths, up to

$$\begin{aligned}\lambda_g^{\text{Ge}} &= \frac{1.24}{0.67}\ \mu\text{m} \\ &= 1.83\ \mu\text{m}.\end{aligned} \tag{12.24}$$

For detecting even deeper into IR, one can use $InSb$, of bandgap $E_g^{InSb} = 0.17\ \text{eV}$, which gives

$$\begin{aligned}\lambda_g^{InSb} &= \frac{1.24}{0.74}\ \mu\text{m} \\ &= 7.3\ \mu\text{m}.\end{aligned} \tag{12.25}$$

Similarly, to detect UV light, we have to use materials of larger bandgap. For example, Z_nS has a bandgap, $E_g^{Z_nS} = 3.54\ \text{eV}$, which yields

$$\begin{aligned}\lambda_g^{Z_nS} &= \frac{1.24}{3.54}\ \mu\text{m} \\ &= 0.35\ \mu\text{m}.\end{aligned} \tag{12.26}$$

Figure 12.16(c) shows the absorption coefficient of various materials as a function of wavelength. Various stoichiometries of InGaAs are very popular for building

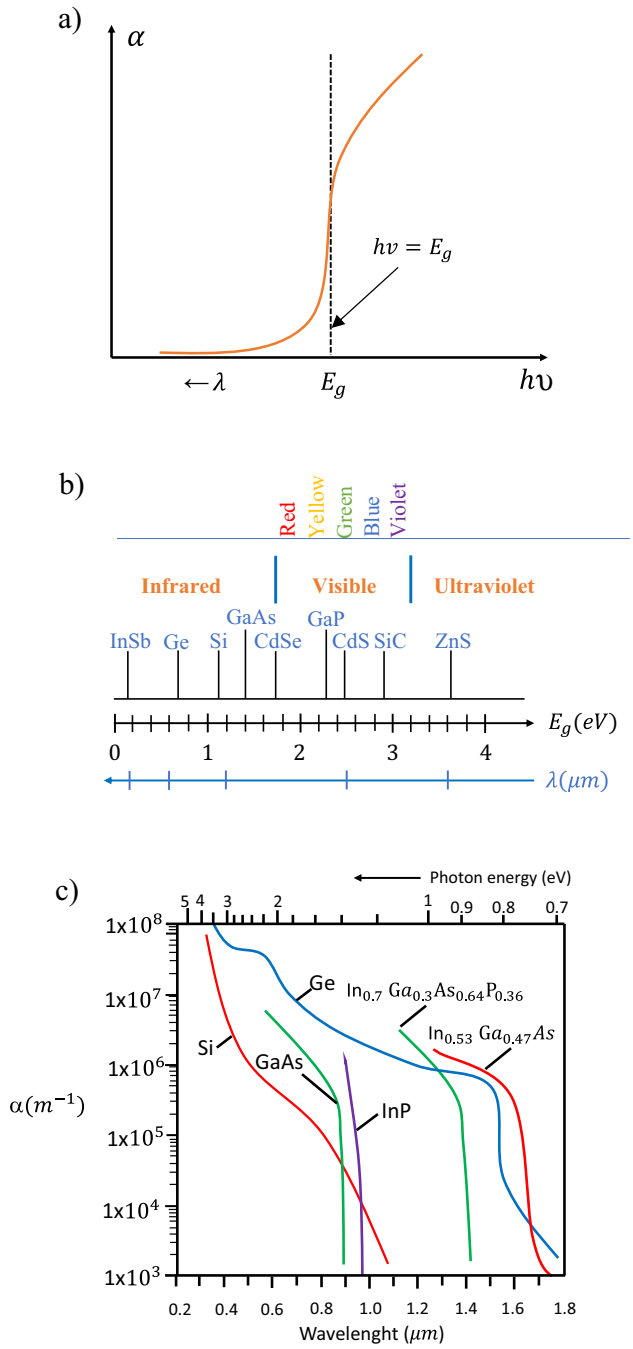

Figure 12.16. (a) Absorption coefficient increases abruptly for energies above the bandgap. (b) Energy bandgap and respective wavelengths for various materials. (c) Wavelength dependence of the absorption coefficient for various materials.

photodetectors in the near infrared. The largest wavelength detectable, corresponding to the bandgap, is sometimes called the *cut-off* wavelength.

Cooling is a valuable procedure to boost the performance of detectors, particularly at long cut-off wavelengths. By cooling, the number of carriers generated thermally goes down. Thermal excitation happens by the incident photon exciting vibrations on the lattice (excites photons) which ultimately increases the temperature in the material. This temperature rise increases the probability of an electron occupying the conduction band. This thermal excitation results in noise (dark current). Since the energy levels in the conduction band are distributed as $e^{-E_g/2k_BT}$ (see section 12.4), this thermal noise is particularly significant for E_g materials, that is, for detection of long wavelengths. Extreme forms of cooling, called *cryogenic* cooling, by, for example, liquid nitrogen ($T = 77$ K) brings the thermal noise essentially to zero.

12.7 P–N junction

A p–n junction is, as the name suggests, the interface between a p-type and n-type semiconductor [5]. P–n junctions are broadly used in semiconductor devices, including diodes, transistor, solar cells, LEDs, and integrated circuits. Although both p-doped and n-doped materials are somewhat conducting, the junction between the two can be depleted of carriers via recombination and, thus, rendered nonconductive, unless voltage bias is applied across the junction. The junction can operate as a *diode*, allowing for current to flow in one direction and not in the other (see section 12.8 on diodes as photodetectors). Figure 12.17 illustrates a junction and its circuit symbol.

Recall that for an intrinsic semiconductor the Fermi level lies in the middle of the bandgap (figure 12.13(a)). The Fermi level is the energy level filled with a probability of 50%. For an n-type semiconductor, the Fermi level is raised closer to the conduction band (figure 12.13(b)). This happens because the majority of the carriers are electrons and are more mobile than the holes, which are trapped. The p-type materials have the Fermi level shifted toward the valence band (figure 12.13(c)).

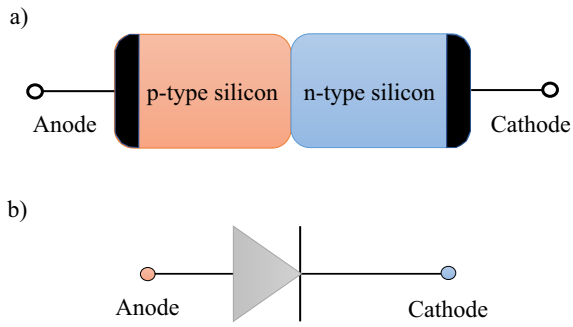

Figure 12.17. (a) A p–n junction formed by connecting a p-type and an n-type Si material. (b) Diode symbol: the base of the triangle corresponds to the p (*anode*) side.

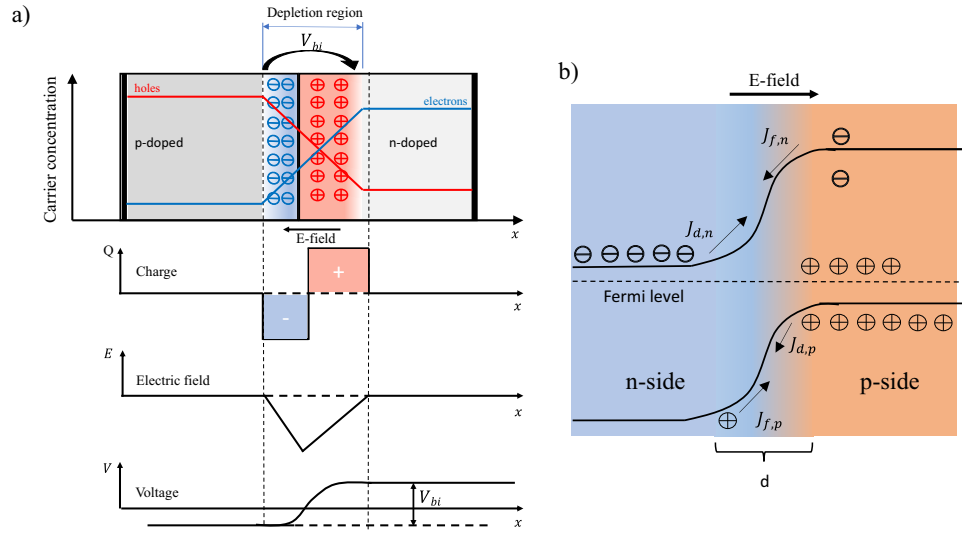

Figure 12.18. (a) A p–n junction in thermal equilibrium with zero-bias voltage applied. Under the junction, plots for the charge density, the electric field, and the voltage are shown. (b) The band diagram for the p–n junction, indicating that the Fermi levels overlap across the two regions. J indicates particle flux, the underscript d indicates diffusion flux, while f stands for "field" (directed) flux due to the electric field **E**. As usual, e and h stand for electrons and holes, respectively. D is the width of the depletion region.

Forward-and reverse-bias operation correspond to placing the positive voltage at the anode and cathode, respectively, and allow the junction to operate as a diode. First, we study the p–n junction in the absence of bias.

12.7.1 Zero bias

Figure 12.18(a) illustrates a p–n junction at thermal equilibrium and zero bias. The free electrons in the n-type material are attracted by the p-side, where they recombine with the holes and neutralize. However, the donor dopants in the n-type material are fixed and remain positive. Conversely, the acceptor dopants in the p-type material remain negatively charged. Thus, at equilibrium, there is a potential difference, known as the *built-in potential*, V_{bi} (see figure 12.18(a)).

The electric field, **E**, generated by charge build-up at the interface tends to oppose the diffusion of both the electrons and holes. Fick's law states that the diffusion flux, say for electrons, J_n, is proportional to the particle concentration gradient,

$$\mathbf{J}_n = -D_n \nabla n(\mathbf{r}) \tag{12.27}$$

where D_n is the diffusion coefficient for electrons and n their concentration. For holes, Fick's law has the analog form, namely,

$$J_{d,p} = -eD_p \frac{dp(x)}{dx}, \tag{12.28}$$

where $J_{d,p}$ is the hole diffusive current (see figure 12.18(b)), flowing from the p- to the n-side, e is the elementary charge, p is the concentration of holes, assumed to only vary in 1D, along x, and D_p is the diffusion coefficient of holes.

The current generated by the electric field E represents a *drift* current, $J_{f,p}$ (figure 12.18(b)) defined as

$$\mathbf{J}_{f,p} = e\mu_p p(x)\mathbf{E}, \tag{12.29}$$

where μ_p is the mobility of holes. At equilibrium, the two currents are equal, that is,

$$e\mu_p p(x)E = eD_p \frac{dp(x)}{dx}. \tag{12.30}$$

Integrating equation (12.30), we obtain

$$\mu_p \int_0^d E\, dx = D_p \int_{p_-}^{p_+} \frac{dp(x)}{p(x)}, \tag{12.31}$$

where d is the width of the depletion region, p_- is the hole concentration in the n-side and p_+ the hole concentration in the p-side. Performing the integrals in equation (12.31), we obtain for the built-in voltage

$$V_{bi} = \frac{D_p}{\mu_p} \ln\left(\frac{p_+}{p_-}\right). \tag{12.32}$$

In equation (12.32), $V_{bi} = \int_0^d E\, dx$ is the built-in voltage (see figure 12.18(a)). In 1905, Einstein derived an expression for the diffusion coefficient of charged particles at thermal equilibrium, as

$$D = \frac{k_B T \mu}{q}, \tag{12.33}$$

where, as usual, k_B is Boltzmann's coefficient, T is the absolute temperature, and q is the charge of the particle. Thus, the built-in voltage can be expressed by combining equations (12.32) and (12.33), as

$$V_{bi} = \frac{k_B T}{e} \ln\left(\frac{p_+}{p_-}\right). \tag{12.34}$$

Equation (12.34) gives an expression for the voltage at equilibrium, when the diffusion and drift currents cancel out for both the holes and electrons.

12.7.2 Forward bias

In *forward* bias, the positive electrode is attached to the p-type material and the negative electrode to the n-type material (see figure 12.19(b)). In this configuration, the positive voltage repels holes from the p-side and the negative voltage repels electrons from the n-side. The overall effect is that the depletion region shrinks. If

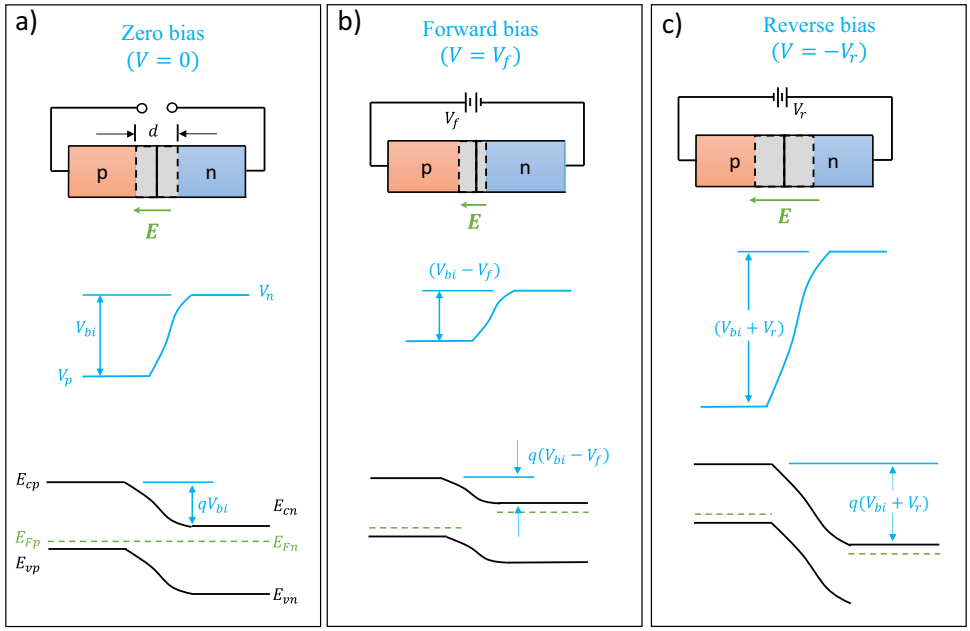

Figure 12.19. p–n junction, voltage, and energy levels for zero-bias (a), forward bias (b), and reverse bias (c).

the forward-bias voltage is progressively increased, the depletion region may become so thin that the built in electric field is not large enough to generate a drift current to cancel the diffusive current. As a result, the overall resistance of the junction decreases. In this *diffusion-dominant* regime, the electrons in the p-region and holes in the n-region eventually recombine, on average, after a distance called *diffusion length,* typically of the order of microns. Note that, although these *minority carriers* penetrate only a short distance in the material, the majority carrier current insures constant charge flow. Thus, in the p-region, the holes travel in the opposite direction to the electrons and, since their charge is also different in sign, contribute to the same current. The converse situation happens in the n-region. Thus, increasing the forward-bias voltage results in a sharp increase in current (see figure 12.20 for the current versus voltage diagram).

12.7.3 Reverse bias

The reverse bias of the p–n junction is achieved by connecting the negative electrode to the p-region and vice versa (figure 12.19(c)). Because the negative electrode tends to pull the holes away from the junction, the depletion region tends to increase in width (a similar effect happens in the n-region). Overall, this phenomenon leads to an increased resistance in the junction, which acts roughly as an insulator. Increasing the reserve bias voltage, that is, applying more negative voltage, yields a high built-in electric field, but without significant increase in the current. At some point, once the electric field intensity reaches a critical value, the p–n junction depleted zone

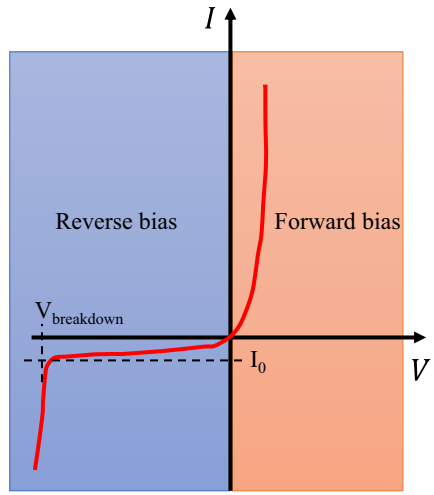

Figure 12.20. Characteristic *I–V* curve for a p–n junction: I_0, reverse saturation current, $V_{\text{breakdown}}$, breakdown (avalanche or Zener) voltage.

'breaks down' and the current begins to flow (figure 12.20). This phenomenon is used in *avalanche* or *Zener* diodes.

12.8 Problems

1. Using the Fermi distribution (equation (12.2b)) show that the probability for an electron to occupy the Fermi level is ½. Find the energy levels for which the probability is 0.1 and 0.9.
2. Calculate the intrinsic carrier concentration for Si at $T = 100$ K, $T = 200$ K, and $T = 300$ K.
3. Calculate the intrinsic carrier concentration for Ge at $T = 100$ K, $T = 200$ K, and $T = 300$ K.
4. Calculate the relative change in intrinsic charge concentration in Si versus Ge, $n_{\text{Si}}/n_{\text{Ge}}$, for a temperature change from $T = 300$ K to $T = 260$ K.

References

[1] Sze S M and Ng K K 2006 *Physics of Semiconductor Devices* (Hoboken, NJ: Wiley)
[2] Nye J F 1984 *Physical Properties of Crystals: Their Representation by Tensors and Matrices* (Oxford: Oxford University Press)
[3] Kittel C 2005 *Introduction to Solid State Physics* (New York: Wiley)
[4] Streetman B G and Banerjee S 2006 *Solid State Electronic Devices* 6th edn (Prentice Hall Series in Solid State Physical Electronics) (Upper Saddle River, NJ: Pearson/Prentice Hall), xviii p 581
[5] Chuang S L 1995 *Physics of Optoelectronic Devices* (Wiley Series in Pure and Applied Optics) (New York: Wiley), xv p 717